Limitations of Short Basalt Fibers Use as an Effective Reinforcement of Polyethylene Composites in Rotational Molding Technology

Joanna Aniśko[1*], Dawid Bartczak[1], Mateusz Barczewski[1]

[1] Poznan University of Technology, Institute of Materials Technology, ul. Piotrowo 3, 61-138 Poznań, Poland
* Corresponding author's e-mail: joanna.anisko@put.poznan.pl

ABSTRACT

The rotational molding technology is becoming more popular and even outstanding some of the conventional polymer processing technologies. The production of polymer composites via this technology is still not described thoroughly. This work discusses the possibilities of obtaining polyethylene composites reinforced with short basalt fibers. Two methods of incorporating the fibrous fillers, dry-blending and through preliminary extrusion, are concerned. The application of the extrusion step to mixed polymer matrix with basalt fiber results in better distribution of basalt fibers than the direct dry blending polymer powder with fiber in the mold. The basalt fibers from rotomolded samples prepared from melt mixed plastic powder significantly reduced their length, leading to a substantial limitation in their reinforcing effect on the polymer matrix. The possible reinforcing effect was evaluated in a mechanical test such as a tensile test and hardness. Optical microscopy helped in the investigation of the distribution of basalt fibers. Not only the physical structure of composites was examined, but also the chemical composition using the Fourier transform infrared spectroscopy. The spectroscopic analysis confirms a properly realized technological process without degradation caused by rotational molding or additional melt blending. The production of good-quality rotomolded composites reinforced with basalt fibers depends on the method of incorporating the fibrous filler.

Keywords: polyethylene; bioPE; rotational molding; composite; mechanical properties

INTRODUCTION

Rotational molding is one of the most dynamically developing technologies for processing thermoplastics, especially in forming thin-walled large-size products [1,2]. The possibility of producing, in one operation, solid products of considerable dimensions and recycling ability after ending their lifetime causes rotomolding gradually displaces products made of laminates based on thermoset resins in the case of products with lower requirements for mechanical performance. The forming process is based on introducing a thermoplastic polymer powder into the mold, rotating on two axes, reflecting the product's outer surface, and then covering it with thermoplastic powder, mainly polyethylene (PE). Dominant effects during forming are sintering, melting, and further densification until a solid layer constitutes

the product [2–4]. Due to the nature of the process, i.e., long-term processing of materials in an oxidizing atmosphere, and the availability of materials used for rotomolding, one of the solutions currently being considered for extending the scope of application by improving selected properties is the use of polymer composites [5]. However, the main problem during the production of composites in the process of one-step forming via rotational molding is the formation of filler agglomerates, phase separation, and insufficient interphase adhesion [6–8].

The experience to date shows that it is possible to manufacture composites in the rotational molding technology by introducing powder and fibrous fillers. The use of each of these groups is associated with a separate group of technological problems and limitations. In the case of introducing fibrous fillers, the increased aspect ratio

causes issues with their dispersion and densification of composite structure, while using polymer powders with improper particle sizes causes difficulties in the sintering and significantly lowers the quality of the internal product surface [8–10]. Moreover, by introducing the particle-shaped filler, while it is possible to obtain favorable effects of increasing stiffness or hardness, the tensile strength or ductility of final products is usually reduced [10].

Many current works describe the possibility of introducing fillers of natural origin [11], including those of waste origin [12,13] or being a solution for the management and utilization of invasive plant species [14,15]. At the same time, it is a well-researched phenomenon that composite materials are strengthened by introducing fibrous fillers with high aspect ratios. Both inorganic and natural fibers have been used in rotational molding technology [16–20]. While from the sustainability point of view, the introduction of natural fibers such as hemp, flax [21], bamboo [22], maple [19], abaca, or banana [20] allowed for the improvement of mechanical properties, there was an additional limitation related to the thermal stability of the fillers. Extending cycle times and the necessity to use higher temperatures for composite materials, resulting from higher viscosity of the filled composition, as well as degradation of lignocellulosic fillers often causing additional porosity effects [23], which compensated for the positive fiber reinforcing effect on polymeric matrix. Moreover, the water absorption of natural filler composites, when composites based on biodegradable polymers are used, may be treated as an advantage which improve the potential biodegradation processes, in case of polyolefin natural composites this effect may lead to additional deterioration of structure and mechanical properties [24–26]. Therefore, the use of inorganic fibers for manufacturing high-performance products is justified and, despite many years of research, still requires further investigation. To improve the adhesion of natural fibers for reinforcing in rotational molding technology, the hydroxylation [14,20,22] or the addition of a coupling agent [27] can be assessed. The additional treatment as silanization of the inorganic fillers, can also be performed to improve polymer-fiber interfacial interactions. In work [28], the hollow glass microspheres were subjected to two-step modification, including hydroxylation and silanization.

The research carried out for powder fillers has shown that using a two-step production process, including preliminary mixing in a molten state, may bring beneficial effects resulting from better filler dispersion in the matrix [10]. In the case of fiber-reinforced composites, the question arises whether the use of a process that takes into account the initial mixing in the extrusion process and subsequent microgranulation or pulverization will not result in an excessive limitation of the length of the fibers, which could result in the loss of their reinforcing efficiency.

In their studies, Gupta and Ramkumar [25] presented the influence of short glass fiber addition on the thermal and rheological properties of LLDPE rotomolded products made by one-step forming. Their analysis showed that the presence of inorganic fibrous filler led to deterioration of processing properties, assessed by melt flow index (MFI) decrease, significant reduction of the viscosity, and increased crystallization temperature of polyethylene matrix. Unfortunately, the insights into the structure of the composites and analysis of fiber distribution and its' influence on mechanical properties were not discussed. Castellanos and co-workers [29] focused on describing the sintering process in polyethylene-glass fibers. They showed that increasing the processing temperature from 200 to 250 °C significantly reduces the number of pores in the structure of composites. This suggests that the use of thermally stable inorganic fibers and the possibility of a more comprehensive selection of temperature conditions may reduce the number of defects observed for composites reinforced with natural fibers. The authors also emphasized the important role of the use of fibers with the appropriate sizing, determining the proper supersaturation of the filler by the molten polymer. Promising studies of applying wollastonite short fibers to produce polyethylene composites by rotomolding were presented by Yuan et al. [30]. The mechanical properties of injection and rotomolded composites showed comparable results in the preliminary mixing of the molten state and pulverization. The authors used fibers with a mean particle size of 16.6 μm and proved that selected mineral fillers with a relatively low aspect ratio and high surface area might effectively reinforce rotomolded composites. Despite the high shearing mixing method (extrusion), the tensile strength was significantly higher than in the dry-blended series, revealing

deterioration of the mechanical properties with increasing filler content.

The major group of rotomolded composites is based on a polyethylene matrix, which can be replaced with bio-based polyethylene since it has the same properties as fossil-based PE but a different synthesis. The bio-polyethylene synthesis starts with the bio-ethanol production from glucose and then the polymerization of ethylene monomer by dehydration [31]. Glucose can be obtained from biological feedstock like sugar cane, sugar beet, starch crops, wheat, and lignocellulosic materials [32]. The bio-polyethylene form Braskem is made out of a sugar cane plant, which can capture CO_2 from the atmosphere. According to Braskem, sugar cane plants capture 2.5 tons of CO_2 on each ton of produced green polyethylene. These properties allow for maintaining the balance of CO_2, which is why this bio-based polyethylene can be named green polymer [31,33].

Taking into account the research described so far, in particular emphasizing the possibility of obtaining a reinforcement effect even by a small length of fibers, it seems reasonable to analyze the influence of the addition of not evaluated basalt fibers on changes in the mechanical properties of biobased polyethylene. The work involved a comparison of two methods of compaction formation (dry blending and melt extrusion) for structurally oriented analyzes of changes in mechanical properties.

EXPERIMENTAL

Materials

The polymer material used for matrix in rotomolded parts is the biobased high-density polyethylene HDPE SHC 7260 I'm Green ® (Braskem, Brazil). The melt flow index of the used matrix is 7.2 g/10 min (190 °C/2.16 kg), and the density of 0.959 g/cm³ according to the producers' data. The minimum biobased content defined by the producer of this grade is 94 %, according to ASTM D6866. The fibrous filler used to prepare composite materials is chopped basalt fibers BF type BCS 13-1/4"-KV02M from Kamenny Vek company (Dubna, Russia), with a diameter of 13 μm, mean fiber length of 6.2 mm, silanization (0.4 wt%) and density of 2.7 g/cm³.

Rotational molding

The process of rotational molding was performed in two different methods:

1) Dry blending

The neat polymer in the form of pellets was ground using a high-speed mill Retsch ZM 200 with a sieve of 500 μm at a 10,000 rpm knife rotational speed. The basalt fibers were introduced in the amount of 2.5, 5, 10, and 20 wt%; they were physically mixed with the previously obtained polymer powder. Materials before rotational molding were dried at 90 °C for 24 h, 100 g of previously prepared physical premixes were introduced into the forms with dimensions of 180×60×60 mm and made of a 2 mm thick steel sheet. The rotational molding process was carried out using the laboratory scale machine: a single-arm shuttle rotational molding machine (REMO GRAF, Poznan, Poland) [11]. The rotational speeds of the horizontal and vertical axes were 15 rpm and 5 rpm. The temperature of the heating chamber was 250 °C, and the time of rotational molding was 30 min; after this time, the molds still in the rotational movement were cooled in a forced air flow station for 20 min.

2) Melt mixing

This method has been enriched with the preliminary step, which was the extrusion process to introduce fiber fillers into the polymer matrix. The extrusion process was carried out on the twin-screw co-rotating extruder Zamak 16/40 EHD (Zamak Mercator, Skawina, Poland) with the highest temperature of 190 °C and a rotational speed of the screws was 100 rpm. The extrudates were cooled in a water bath and, after this, pelletized. The pellets were further pulverized using the high-speed mill Retsch ZM 200 equipped with the 500 μm sieve and a rotational speed was 10,000 rpm. The prepared composite powder was then subjected to rotational molding in the same conditions as the dry-blended method.

The dry-blended samples are named bioPE, 2.5% BF, 5% BF, 10% BF, and 20% BF, the melt-mixed samples have the additional suffix "ex".

Characterization tests

Fourier transform infrared spectroscopy

The chemical structure of obtained composites was investigated using the FTIR in ATR mode. The measurement was carried out using

the Jasco FT/IR-4600 (Tokyo, Japan) at scanning resolution 4 cm^{-1}, in the range of wavenumber 4000–400 cm^{-1}, and the number of scans was 64.

Optical microscopy

The optical microscope Levenhuk DTX 500 LCD Digital Microscope (Warsaw, Poland) was used to investigate the structure of the cryo-fractured cross-section of samples. The microscope OPTA-TECH SK (Warsaw, Poland) connected with camera Meiji Techno HD2600T was used to obtain microscopic images of neat bioPE powders and composite powders. This equipment allowed to investigate the length of basalt fiber before and after processing. The computer software adjusted to the microscope made it possible to measure these dimensions with an accuracy of 0.01 mm. The minimum number of measurements for each of the dimensions is 50. To obtain separated fibers after processing, the rotomolded samples were subjected to incineration.

Calcination

To obtain the residue after combustion according to the standard PN-EN ISO 1172 approximately 2 g of rotomolded parts were subjected to incineration at 600 °C for 3 h. The used furnace was SNOL 22/1100 LHM01. After incineration, the residues were used to determine the actual content of the introduced filler in the rotomolded parts. The percentage of inorganic residue fibers is an average value of two measurements.

Mechanical properties

The mechanical properties of rotomolded parts were evaluated using a static tensile test. The Young modulus, tensile strength, and elongation at break were determined based on the standard PN-EN ISO 527-1 adapted to rotomolded samples using the universal testing machine Zwick Roell Z010 (Ulm, Germany). At least 7 samples 100 mm long, 10 mm wide, and approximately 3 mm thick, cut from the side walls of the rotomolded parts, were subjected to this test with the speed of crosshead 1 mm/min during Young modulus determination (up to elongation of 0.2%) and 10 mm/min during the rest of the test.

Brinell hardness test was performed using the hardness testing machine KB Prüftechnik 150R

according to the standard ISO 2039. The value of hardness is the average value of 10 measurements.

Melt flow index (MFI)

The melt flow index measurement was carried out to investigate the processing properties using the plastometer Dynisco LMI 4004 according to standard ISO 1133; the parameters were 190 °C and 2.16 kg.

Thermomechanical analysis (DMA)

The dynamic mechanical properties were obtained using the rheometer Anton Paar MCR 301 (Graz, Austria) with SRF accessory in a torsion mode operating at a 1 Hz frequency in the temperature range 25–100 °C, and the heating rate was 3 °C/min. The samples used for DMA measurement have dimensions 10×50 mm. Apart from the dynamic mechanical properties, the effectiveness of the filler C was determined using the following formula [34]:

$$C = \frac{(\frac{G'_{30}}{G'_{100}})_{composite}}{(\frac{G'_{30}}{G'_{100}})_{matrix}} \qquad (1)$$

where: G'_{30} is the storage modulus at 30 °C, and G'_{100} is the storage modulus at 100 °C [35].

The brittleness was measured using the Brostow et al. formula [36]:

$$B = \frac{1}{\varepsilon \cdot G'_{30}} \qquad (2)$$

where: ε is the elongation at break determined at a speed of 10 mm/min during the tensile test [%], and G'_{30} is the storage modulus at 30 °C.

RESULTS AND DISCUSSION

Structural analysis

The results of the FTIR analysis are presented in Figure 1. The absorption bands visible in FTIR spectra are characteristic of low-density polyethylene. The most distinct absorption bands related to the symmetrical and asymmetrical stretching vibrations of the C-H bonds occurring in the main polyethylene chain are visible at 2845 cm^{-1} and 2915 cm^{-1}. The 1465 cm^{-1} absorption peak is connected with the C-H bond in polymer structure [37]. Besides the characteristic band peaks for

polyethylene, the peak at approximately 1100 cm^{-1} can be distinguished; it represents SiO$_2$ absorption band characteristic for basalt fibers [38]. The silicon dioxide (SiO$_2$) constitutes approximately 50 wt% of basalt fibers mass [39]. The intensities of these peak increase with the rising number of basalt fibers in composites, and these intensities are higher in spectra of melt-mixed samples. In the spectroscopy measurements samples were placed the outer surface of rotomolded parts towards the detector. The higher intensities of SiO$_2$ peak suggest that the distribution of basalt fibers is better and this behavior occurs in melt-mixed samples. In order to neglect the negative effect of the melt processing on polymer structure, the evaluation of FTIR spectra in the range of carbonyl bands representation was evaluated (1650–1850 cm^{-1}). The presence of this peak can imply that some degradation occurs in the polymer matrix [40]. There was no distinct absorption band in mentioned range, which allows for omitting the influence of thermal or thermooxidative degradation on mechanical properties.

The distribution of basalt fibers in the polymeric matrix is insufficient in dry-blended samples. Most of the introduced basalt fibers are located near the inner surface of the rotomolded part. This effect is caused by the high difference in densities and size of the polymer matrix and introduced filler, which is almost three times higher for basalt fibers. The rotating around the horizontal and vertical axis of the mold at low rotational speeds causes the migration of basalt fibers far from the mold walls. Considering only the bed flow of the particles in the mold's uniaxial rotating movements, there are 5 different flow regimes: slipping, avalanching, rolling, cataracting, and centrifuging [41]. When used particles have different properties, such as density, size, shape, or surface roughness, segregation may occur caused by the clustering of similar particles [42]. In this case, not only does the segregation of particles in bed flow by their densities causes the migration of basalt fibers to the outer surface, but also the PE particles tends to go to the mold surface because of their size and shape and then quick melting of polyethylene powders on the mold wall occurs. The melting of the polymeric particles can change the movements of powder from slipping to avalanching. In avalanching flow, the particles uniformly flow near free surfaces, these particles are the basalt fiber, and this movement limits the ability to mix the fibers with the polymer matrix [2,41]. Mixing fiber filler is also difficult because of the low-shear rates characteristic of the rotational molding process [10]. In these conditions, the polymer not subjected to non-newtonian melt flow region is characterized by high viscosity, revealing hindrance with fully infusing basalt fibers. When as a pre-processing dry blending is applied for the preparation of the natural fibers with polymeric powder premixes, the final distribution of the filler was reported to be uniform in the volume of the rotomolded part [14,23,27]. On the other hand, the products manufactured from the melt-mixed composition showed the homogenous distribution of basalt fibers; only the samples with 2.5 wt% BF showed fillers located closer to the outer surface. The advantage of using the preliminary melt mixing process is improved dispersion of the fibers in a polymer matrix, which is connected with the occurrence of high shear rates. The remaining bubbles in the composite can be distinguished in the images of fractured samples (Fig. 2). The high concentration of pores is observed in structures of
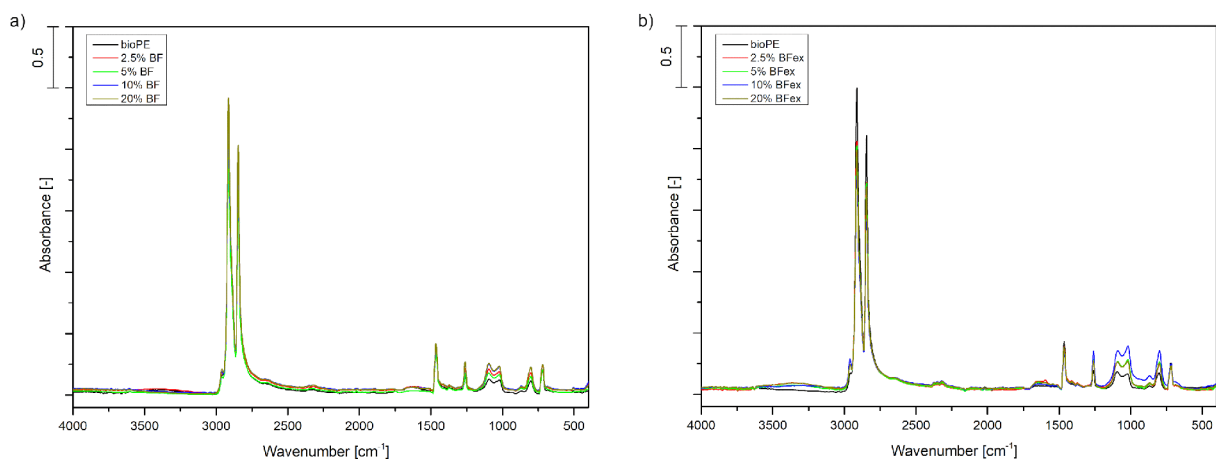

Fig. 1. FTIR spectrum of rotomolded parts dry-blended (a) and melt mixed (b)
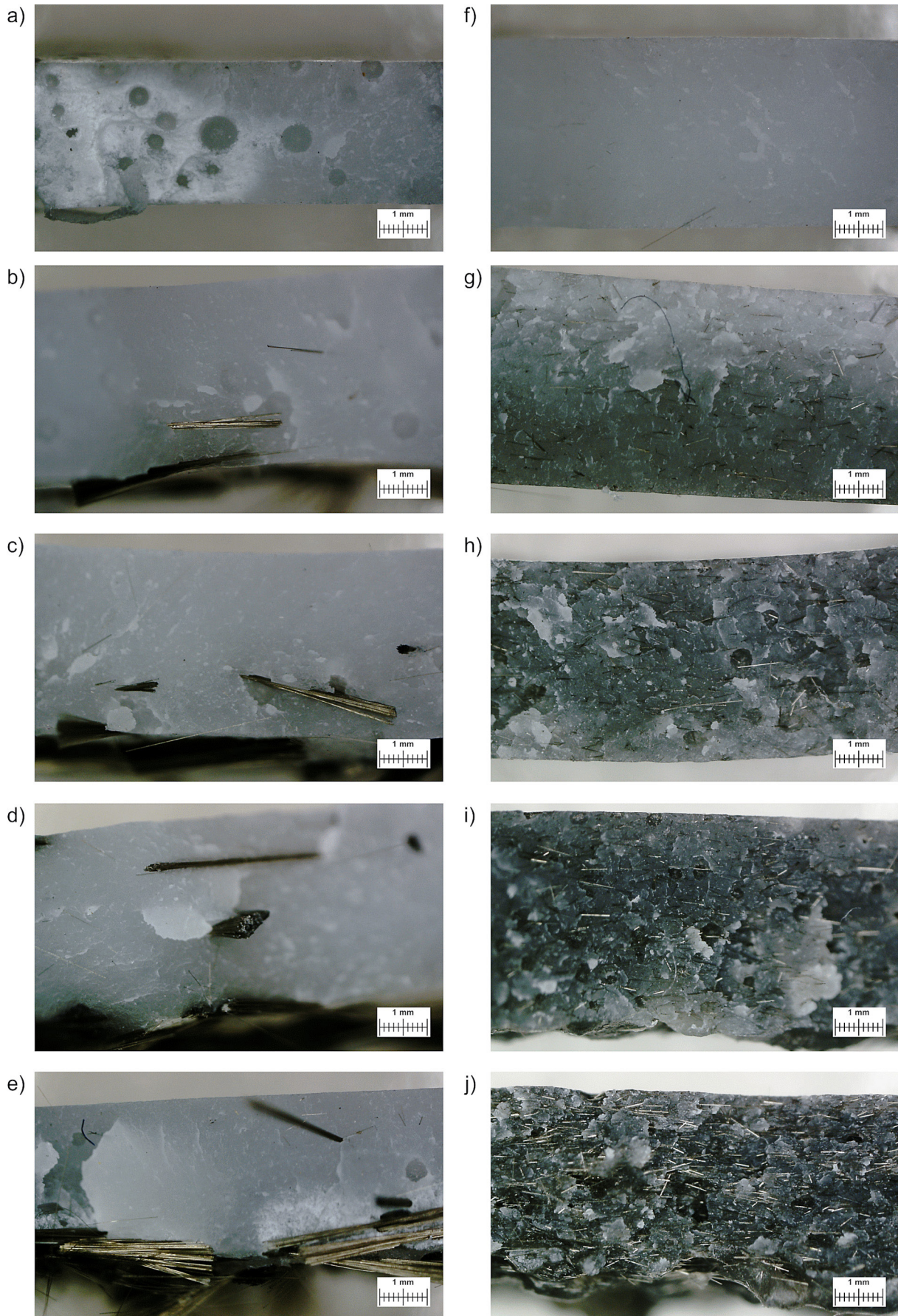
a)

f)

b)

g)

c)

h)

d)

i)

e)

j)

Fig. 2. Optical microscope images of fractured rotomolded samples prepared by dry blending (a, b, c, d, e) and melt mixing (f, g, h, i, j) arranged from top to bottom with the increase in basalt fibers content

an unfilled dry-blended bioPE sample, as well as in some composite dry-blended samples. In the melt-mixed series, the pores are visible for the 5, 10 and 20 wt% of basalt fibers near the fibers. This means that the presence of pores in melt-mixed samples can be connected with the release of the residual moisture entrapped in filler or thermal degradation of the silane sizing during long-time processing.

The preliminary grinding of melt-mixed composites with fiber fillers resulted in pulling out basalt fiber from the polymer matrix. Figure 3 presents microscopic images of polyethylene powders after grinding. The amount of torn fibers from the polymer matrix increased gradually with the increase in basalt fibers in composite materials. The

inorganic fibers and nonpolar polyethylene create a weak bond between them; despite the application of silane sizing of the BF. The different modifications of the fibers, such as dopamine hydrochloride [35], may decrease the intensity of the mentioned effect to improve the interfacial adhesion. Figures 3a and 3b present neat polyethylene powder images to compare composite powder materials' morphology. All powder particles have irregular shapes, but the particles of neat bioPE and bioPEex have much smoother surfaces. The visual effect of sharp edges can be caused by the presence of basalt fibers.

The rotomolded parts were subjected to pyrolysis to investigate the amount of residue basalt fibers. Table 1 presents the weight percentage
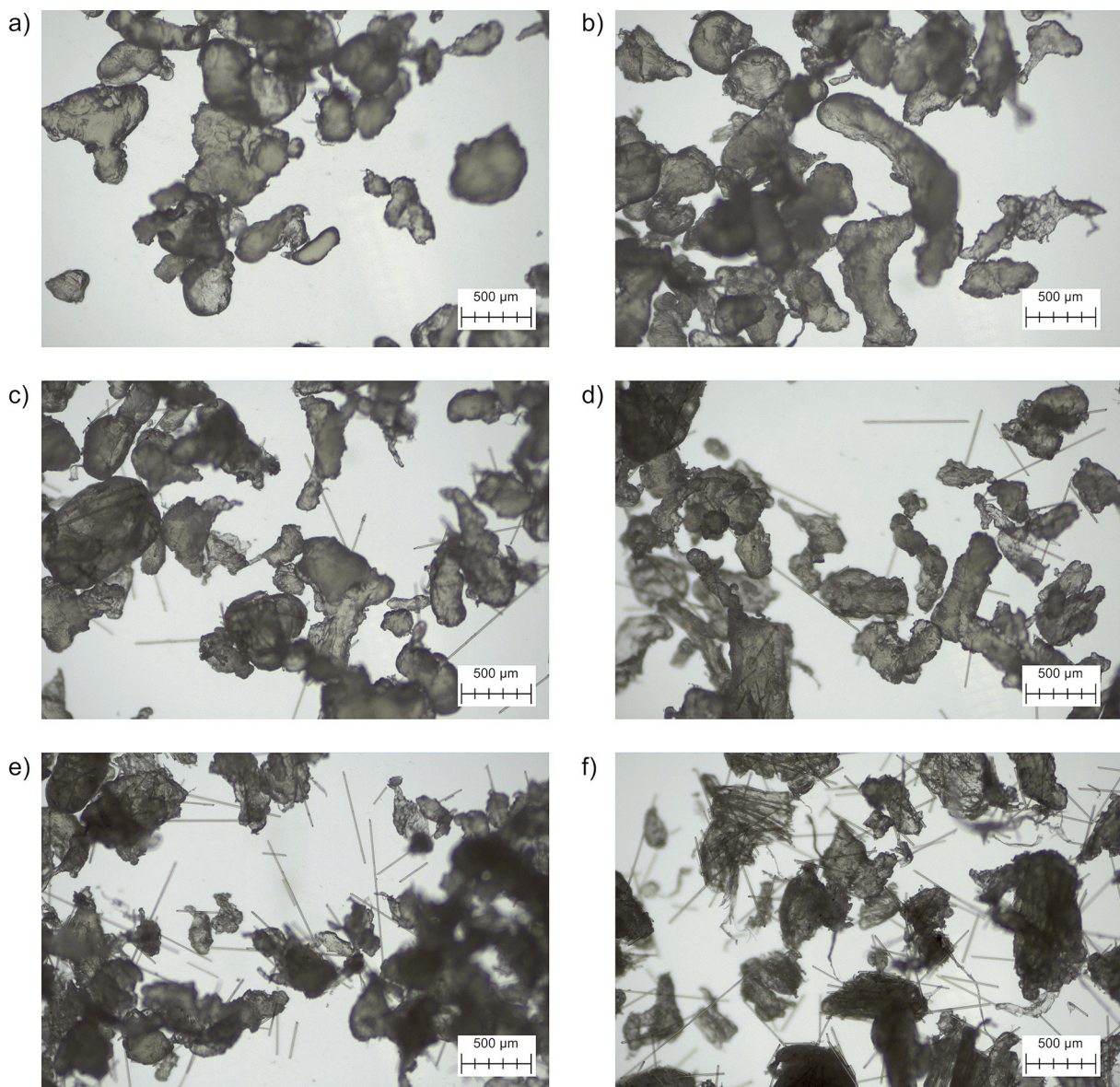

Fig. 3. Optical microscope images of powder materials: bioPE (a), bioPEex (b), 2.5% BFex (c), 5% BFex (d), 10% BFex (e), 20% BFex (f)

Table 1. The thermally stable residue after pyrolysis, which described the authentic content of inorganic filler

Sample	Content after pyrolysis [wt%]
bioPE	0.08
2.5% BF	1.27
5% BF	2,49
10% BF	9.08
20% BF	11.90
bioPEex	0.07
2.5% BFex	2.22
5% BFex	4.68
10% BFex	10.04
20% BFex	19.52

Table 2. Length of the remaining basalt fibers after pyrolysis of rotomolded samples

Sample	Fibers length [mm]
Basalt fibers	3.251 ± 0.288
2.5% BF	1.804 ± 0.947
5% BF	1.894 ± 0.959
10% BF	2.696 ± 0.739
20% BF	2.782 ± 0.756
2.5% BFex	0.204 ± 0.093
5% BFex	0.213 ± 0.095
10% BFex	0.237 ± 0.099
20% BFex	0.306 ± 0.118

of residue matter after annealing at 600 °C. The residue content after pyrolysis for dry-blended samples does not reflect the number of introduced basalt fibers. The not regular distribution of fibers results in not even weight percentage content; this is seen in dry-blended samples. On the other hand, the melt-mixed composites have the amount of residue closely related to the number of introduced fibers.

The residues after pyrolysis were also subjected to further investigation to describe the pre-processing step conditions on the geometry of the fiber. The optical microscopy images allowed to measure the fibers' length and describe their visual appearance. In Figure 4, basalt fibers before processing are presented; the length of these fibers is 3.25 ± 0.29 mm. The unprocessed fibers and fibers used in dry-blended samples have many fibers connected. The insufficient saturation of fibers with polymer matrix via dry blending method results in the still clustering effect of the fibers. As previously mentioned, low shear rates occurring in rotational molding technology are not enough to homogenously distribute the basalt fibers and achieve the effect of proper saturation of the inorganic filler by molten polymer with high viscosity. Application of the preliminary step in which fibers were introduced into a polymer matrix via extrusion resulted in better distribution of fibers in final rotomolded parts and better saturation of fibers. The melt mixing method has one big disadvantage: the fibers' length decreased significantly. The length of fibers after the dry blending method are shorter by approximately 1 mm in comparison to unprocessed ones. However, the fibers after melt mixing are shorter by 3 mm, which is 93% reduction in length. All fibers' lengths before and after processing are presented in Table 2.

Mechanical and thermomechanical analysis

The mechanical properties of rotomolded parts are strongly correlated with the distribution of added basalt fibers. The Young modulus does not change significantly with the increase of the filler. The difference between the highest and lowest modulus of elasticity is 13% of the average modulus for dry-blended samples and 25% of the average for melt-mixed composites. No significant stiffening was observed in the dry-blended and melt-mixed series. The uneven distribution of fibers in dry-blended samples has no reinforcing effect on the composite structure. Even though the fibers are better distributed in melt-mixed composites, there is no reinforcing effect either. We can observe the slightest increase in modulus of elasticity which also causes the decrease in tensile strength. This kind of behavior is characteristic of particle-reinforced composites. Polyethylene composites reinforced with fibers have an enhanced modulus and tensile strength [43]. The polyethylene composites reinforced with glass fiber in a length of 4 mm exhibit an increase in elasticity modulus and tensile strength with the rising filler content [44]. The decrease in elongation value at the break is observed for dry-blended and melt-mixed samples. There is the slightest increase in elongation after adding 2.5 wt% BF for materials manufactured with the preliminary extrusion step. Overall elongation at the break is higher for these samples than for dry-blended.

In Figure 6 is presented hardness of rotomolded parts, which improved with the increase in basalt fiber content. There is a slight increase in hardness in melt-mixed samples. This can be correlated with the better distribution of rigid inorganic fibers, including their presence in the
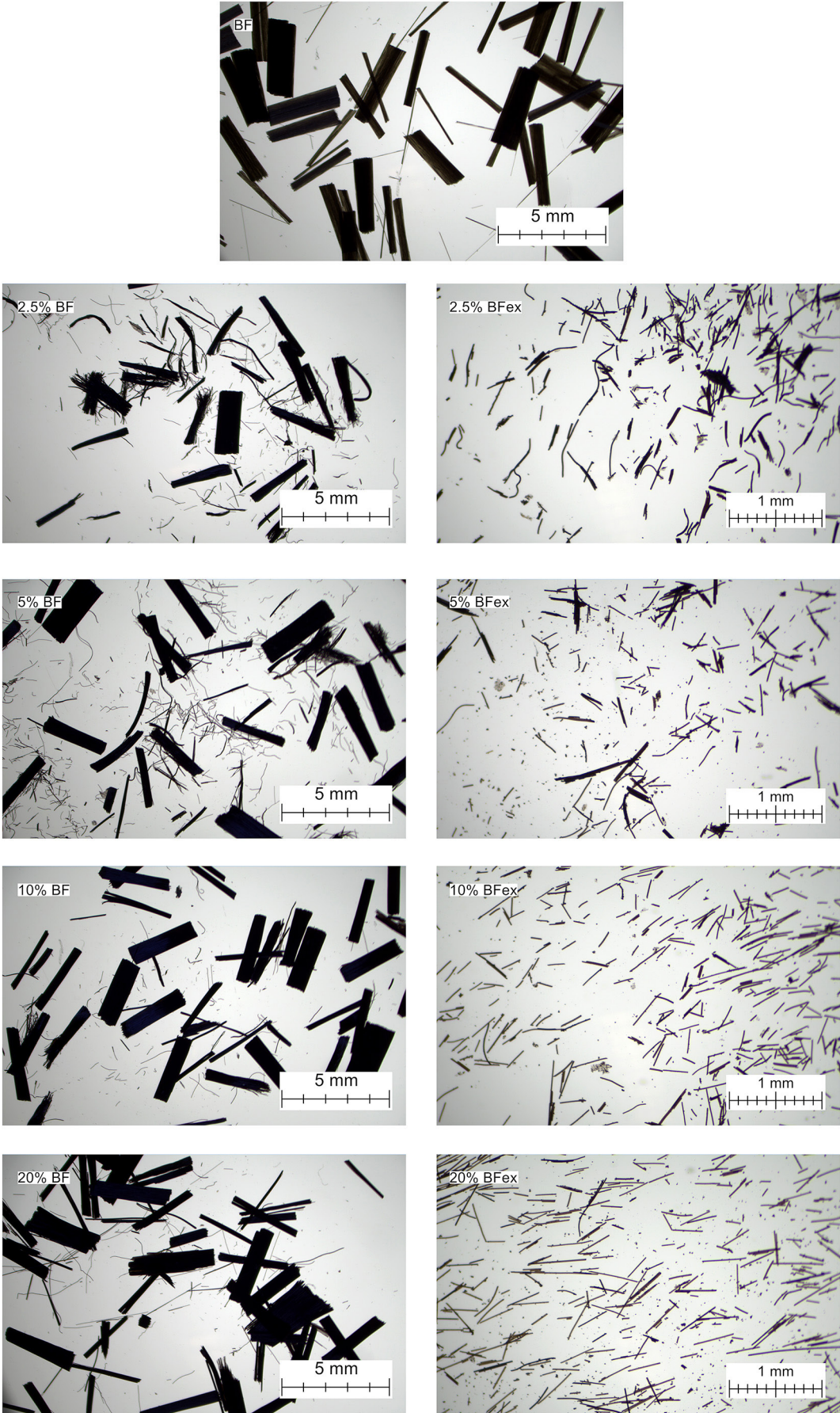
Fig. 4. Basalt fibers before and after processing via rotational molding (left side)
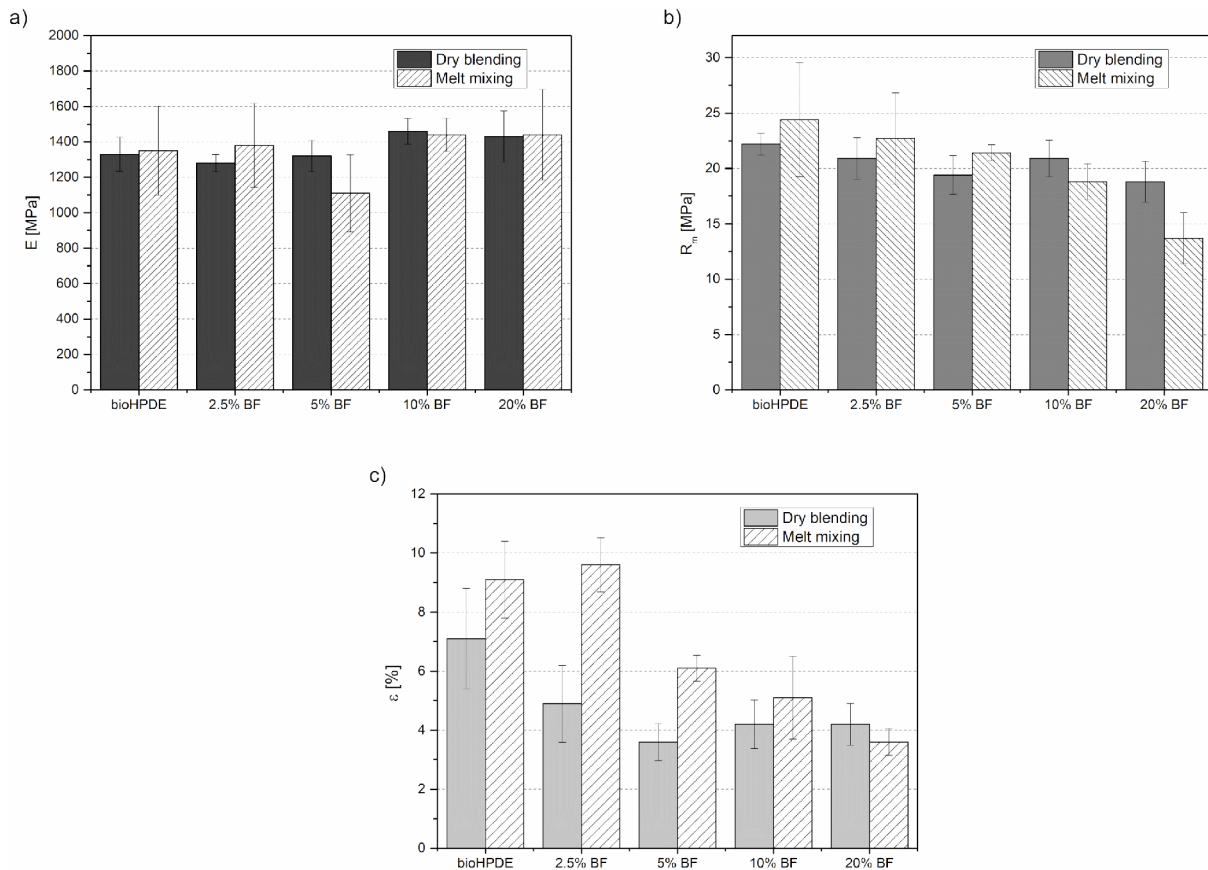and extrusion followed by rotational molding (right side)

Fig. 5. The mechanical properties from a tensile test for dry-blended and melt-mixed samples
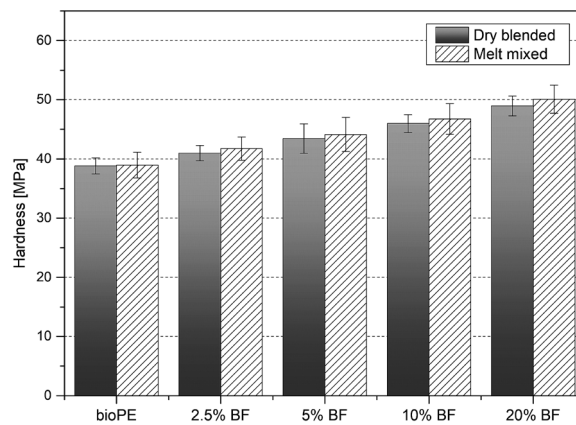

Fig. 6. Hardness of dry-blended and melt-mixed samples

surface area of the composite part. In the dry blended samples the basalt fibers are located near to the inner surface and the hardness test was performed by pressing the indenter from the outer surface of samples.

Figure 7 presents the results of thermomechanical tests performed by DMA. The diagrams of storage modulus (G') and damping factor (tanδ) as a function of temperature for a series of materials produced with the use of two different mixing

methods of polymer-filler composition for the rotational molding process were compared. Considering the slight possibility of the influence of inorganic fibers, remaining inactive towards the polyethylene matrix, and the proven risk of degradation effects, the temperature range was narrowed down to 30–100 °C, without considering changes of γ- and β-relaxations of polyethylene [45]. This range allowed to determine the influence of inorganic filler on the thermomechanical
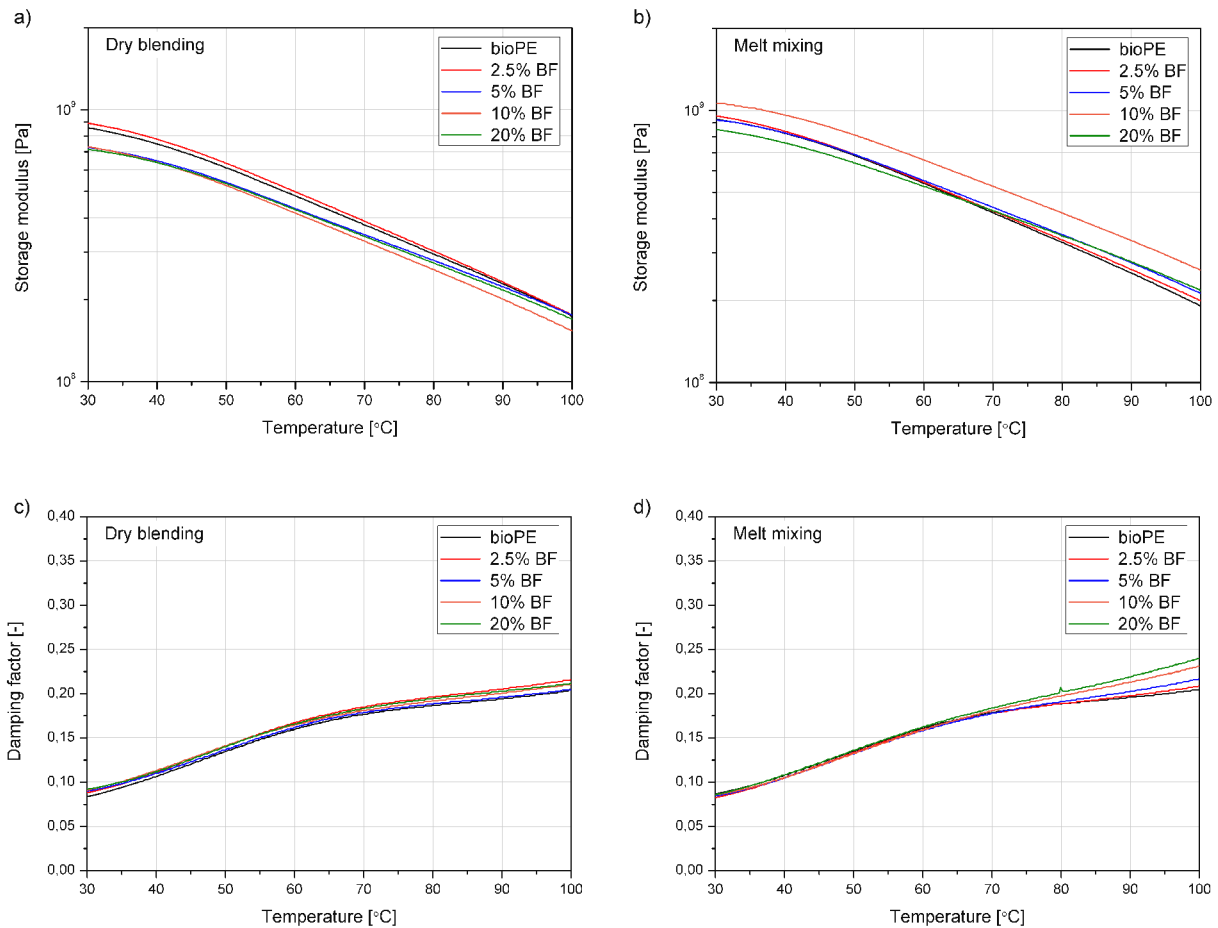
Fig. 7. Thermomechanical curves obtained by DMA; storage modulus
(G') and damping factor (tanδ) vs. temperature (T)

stability of the composites. Storage modulus results are in agreement with static tensile measurements of elastic modulus. The introduction of fillers did not cause significant changes in increasing the stiffness of the material. Interestingly, the G' values recorded for dry-blended samples decreased gradually along with the increased amount of filler. At the same time, the melt-mixed series showed almost no influence of the filler on storage modulus, except 10 wt% BF series. The lack of significant changes to the damping factor of composites, made using only physical mixing before processing, is understandable, taking into account only the surface distribution of the filler in the matrix on the internal part wall. For the melt-mixed series, a gradual increase in the value of tanδ is observed in the upper-temperature range, above the α-relaxation temperature [45]. The observed microporosity may overcome this noted in the interfacial area around the fibers.

The storage modulus values for each of the samples at 30 °C and 100 °C to calculate the effectiveness of the filler *C* and brittleness (B) of dry-blended and melt-mixed composites. The results are summarized in Table 3. The filler interaction efficiency is based on the determination of the *C* coefficient. According to the literature [34], the lower the *C* coefficient, the greater the effectiveness of the filler in the polymer matrix. The values of the *C* presented in Table 3 indicate that the highest efficiency of the filler on the thermomechanical properties of dry-blended composites was found for samples with 5 wt% of basalt fibers (0.84). For composites mixed in the melt state, the highest filler efficiency was achieved for a sample with a 20 wt% of basalt fiber content (0.80), *C* factor decreases in both cases of preparing rotationally molded composites. Still, for the melt-mixed samples, this coefficient is slightly lower, so it can be stated that, in this case, the effectiveness of the influence of the filler is higher. The B-factor calculations presented in the paper may differ from data obtained with the method presented initially by Brostow [36], while the G modulus was used instead of E, and the value of the strain at break was tested with a traverse speed of 10 mm/min.

Table 3. The brittleness and effectiveness of the filler measured using equations (1) and (2)

Sample		Effectiveness of the filler C [-]	Brittleness B [% Pa/10^{10}]
Dry-blended	bioPE	-	1.64
	2.5% BF	1.03 ± 0.07	2.29
	5% BF	0.84 ± 0.24	3.82
	10% BF	0.96 ± 0.31	3.26
	20% BF	0.86 ± 0.17	3.33
Melt-mixed	bioPEex	-	1.18
	2.5% BFex	0.98 ± 0.10	1.09
	5% BFex	0.89 ± 0.07	1.78
	10% BFex	0.84 ± 0.04	1.85
	20% BFex	0.80 ± 0.06	3.27

Table 4. Melt flow index of materials formed during rotational molding

Sample	Melt flow index [g/10 min]
bioPEex	8.94 ± 0.22
2.5% BFex	6.87 ± 0.18
5% BFex	5.95 ± 0.31
10% BFex	4.66 ± 0.15
20% BFex	4.06 ± 0.11

molding technology since the preferred MFI for materials used in rotational molding should be between 2 and 8 g/10 min [48].

CONCLUSIONS

The conducted research allowed to state that despite the high potential of the filler, the technological aspect related to the specific process conditions during rotational molding may make it difficult to obtain effective reinforcement by inorganic fibers. The good distribution of these fillers is a crucial aspect, but it is difficult to obtain; in the case of dry-blended composites, all of the fillers are placed on the inner surface of samples which can be seen on the microscopic images. A better distribution may be obtained by the application of the preliminary step in which the fillers were melt-mixed with a polymer matrix. However, investigations have shown that for both composition pre-processing methods applied prior to the rotomolding process, the effectiveness of the reinforcement by the fibers is reduced. These phenomena, however, in both cases have a different origin. The dry-blending systems showed phase separation and insufficient fiber supersaturation. In the second case, i.e., composites made of micrometric powders produced in the extrusion process were characterized by a reduction in the length of basalt fibers, which lose aspect ratio, it allows for efficient stress transfer and strengthens the polymer. The analysis of the thermomechanical parameters also confirms this behavior.

Acknowledgments

However, it should be noted that this multi-criterion parameter is not an actual physical feature in its interpretation but is an empirically tested qualitative comparative criterion. Therefore, the data cannot be correlated with other data in the literature and have been discussed for comparative purposes. The results described using parameter B show that the samples lose their ductility with the increasing share of the filler. Composites made with preliminary physical mixing show higher brittleness. This phenomenon is related to the increased negative effect of insufficient filler dispersion in the matrix on the storage modulus. The test results are consistent with those obtained in previous studies, both in the case of composites with fibrous as well as particle-shaped fillers [35, 46].

The melt flow index of neat polyethylene provided by the supplier is 7.2 g/10 min; this value was insignificantly increased after preliminary melt processing. Therefore, it can be stated that applied extrusion and milling conditions did not provoke degradation effects on polyethylene. It is different in the case of composite materials; the increasing amount of basalt fibers decreased the MFI, which is correlated with the increase in the viscosity of obtained materials. Adding basalt fibers into a polyethylene matrix can cause limitations in the mobility of polymeric matrix macromolecules, leading to a rise in viscosity [47]. The value of MFI for the sample with the highest content of basalt fibers decreases by 50% of the initial value of MFI for neat bioPE. Even if the noted difference in MFI values between non-filled polyethylene and composite series is significant, it is also in the acceptable range according to the requirements for rotational

REFERENCES

1. Rao MA, Throne JL. Principles of rotational molding. Polymer Engineering and Science. 1972;12(4):237–64.

2. Crawford RJ, Throne JL. Rotational molding technology. New York. 2002. 327 p.

3. Hamidi A, Farzaneh S, Nony F, Ortega Z, Khelladi S, Monzon M, et al. Modelling of sintering during rotational moulding of the thermoplastic polymers. International Journal of Material Forming. 2016;9(4):519–30.

4. Ogila KO, Shao M, Yang W, Tan J. Rotational molding: A review of the models and materials. Express Polymer Letters. 2017;11(10):778–98.

5. Głogowska K, Pączkowski P, Samujło B. Study on the Properties and Structure of Rotationally Moulded Linear Low-Density Polyethylene Filled with Quartz Flour. Materials. 2022;15(6):2154.

6. Yan W, Lin RJT, Bhattacharyya D. Particulate reinforced rotationally moulded polyethylene composites – Mixing methods and mechanical properties. Composites Science and Technology. 2006;66(13):2080–8.

7. Höfler G, Lin RJT, Jayaraman K. Rotational moulding and mechanical characterisation of halloysite reinforced polyethylenes. Journal of Polymer Research. 2018;25(6):132.

8. Baumer MI, Leite JL, Becker D. Influence of calcium carbonate and slip agent addition on linear medium density polyethylene processed by rotational molding. Materials Research. 2013;17(1):130–7.

9. Cisneros-López EO, Pérez-Fonseca AA, González-García Y, Ramírez-Arreola DE, González-Núñez R, Rodrigue D, et al. Polylactic acid-agave fiber biocomposites produced by rotational molding: A comparative study with compression molding. Advances in Polymer Technology. 2018;37(7):2528–40.

10. Aniśko J, Barczewski M, Piasecki A, Skórczewska K, Szulc J, Szostak M. The Relationship between a Rotational Molding Processing Procedure and the Structure and Properties of Biobased Polyethylene Composites Filled with Expanded Vermiculite. Materials. 2022;15(17):5903.

11. Barczewski M, Szostak M, Nowak D, Piasecki A. Effect of wood flour addition and modification of its surface on the properties of rotationally molded polypropylene composites. Polimery. 2018;63(11/12):772–84.

12. Głogowska K, Majewski Ł, Gajdoš I, Mitaľ G. Assessment of the Resistance to External Factors of Low-Density Polyethylene Modified with Natural Fillers. Advances in Science and Technology Research Journal. 2017;11(4):35–40.

13. Andrzejewski J, Krawczak A, Wesoły K, Szostak M. Rotational molding of biocomposites with addition of buckwheat husk filler. Structure-property correlation assessment for materials based on polyethylene (PE) and poly(lactic acid) PLA. Composites Part B: Engineering. 2020;202(May).

14. Ortega Z, Romero F, Paz R, Suárez L, Benítez AN, Marrero MD. Valorization of invasive plants from macaronesia as filler materials in the production of natural fiber composites by rotational molding. Polymers. 2021;13(13).

15. Suárez L, Ortega Z, Romero F, Paz R, Marrero MD. Influence of Giant Reed Fibers on Mechanical, Thermal, and Disintegration Behavior of Rotomolded PLA and PE Composites. Journal of Polymers and the Environment. 2022;

16. Ghanem Z, Šourkova HJ, Sezemsky J, Špatenka P. The Effect of Plasma Treatment of Polyethylene Powder and Glass Fibers on Selected Properties of Their Composites Prepared via Rotational Molding. Polymers. 2022;14(13):2592.

17. Szostak M, Tomaszewska N, Kozlowski R. Mechanical and Thermal Properties of Rotational Molded PE/Flax and PE/Hemp Composites. In 2019. p. 495–506.

18. Abhilash SS, Singaravelu DL. Effect of Fiber Content on Mechanical and Morphological Properties of Bamboo Fiber-Reinforced Linear Low-Density Polyethylene Processed by Rotational Molding. Transactions of the Indian Institute of Metals. 2020;73(6):1549–54.

19. Hanana FE, Rodrigue D. Rotational molding of self-hybrid composites based on linear low-density polyethylene and maple fibers. Polymer Composites. 2018;39(11):4094–103.

20. Ortega Z, Monzón MD, Benítez AN, Kearns M, McCourt M, Hornsby PR. Banana and Abaca Fiber-Reinforced Plastic Composites Obtained by Rotational Molding Process. Materials and Manufacturing Processes. 2013;130614085148001.

21. Szostak M, Tomaszewska N, Kozlowski R. Mechanical and Thermal Properties of Rotational Molded PE/Flax and PE/Hemp Composites. In 2019. p. 495–506.

22. Abhilash SS, Singaravelu DL. Effect of Fiber Content on Mechanical and Morphological Properties of Bamboo Fiber-Reinforced Linear Low-Density Polyethylene Processed by Rotational Molding. Transactions of the Indian Institute of Metals. 2020;73(6):1549–54.

23. López-Bañuelos RH, Moscoso FJ, Ortega-Gudiño P, Mendizabal E, Rodrigue D, González-Núñez R. Rotational molding of polyethylene composites based on agave fibers. Polymer Engineering & Science. 2012;52(12):2489–97.

24. Yew GH, Mohd Yusof AM, Mohd Ishak ZA, Ishiaku US. Water absorption and enzymatic degradation

of poly(lactic acid)/rice starch composites. Polymer Degradation and Stability. 2005;90(3):488–500.

25. Wang B, Panigrahi S, Tabil L, Crerar W. Pre-treatment of Flax Fibers for use in Rotationally Molded Biocomposites. Journal of Reinforced Plastics and Composites. 2007;26(5):447–63.

26. Kufel A, Kuciel S. Hybrid Composites Based on Polypropylene with Basalt/Hazelnut Shell Fillers: The Influence of Temperature, Thermal Aging, and Water Absorption on Mechanical Properties. Polymers. 2019;12(1):18.

27. Robledo-Ortíz JR, González-López ME, Rodrigue D, Gutiérrez-Ruiz JF, Prezas-Lara F, Pérez-Fonseca AA. Improving the compatibility and mechanical properties of natural fibers/green polyethylene biocomposites produced by rotational molding. Journal of Polymers and the Environment. 2020; 28(3): 1040–9.

28. Stagnaro P, Utzeri R, Vignali A, Falcone G, Iannace S, Bertini F. Lightweight polyethylene-hollow glass microspheres composites for rotational molding technology. Journal of Applied Polymer Science. 2021;138(5):1–16.

29. Castellanos D, Martin PJ, Butterfield J, McCourt M, Kearns M, Cassidy P. Sintering and Densification of Fibre Reinforcement in Polymers during Rotational Moulding. Procedia Manufacturing. 2020;47:980–6.

30. Yuan X, Easteal AJ, Bhattacharyya D. Mechanical performance of rotomoulded wollastonite-reinforced polyethylene composites. International Journal of Modern Physics B. 2007;21(7):1059–66.

31. de Andrade Coutinho PL, Morita AT, Cassinelli LF, Morschbacker A, Werneck Do Carmo R. Braskem's Ethanol to Polyethylene Process Development. Catalytic Process Development for Renewable Materials. 2013;149–65.

32. Mendieta CM, Vallejos ME, Felissia FE, Chinga-Carrasco G, Area MC. Review: Bio-polyethylene from Wood Wastes. Journal of Polymers and the Environment. 2020;28(1):1–16.

33. Brito GF, Agrawal P, Araújo EM, Mélo TJA De. Polylactide / Biopolyethylene Bioblends. 2012;22:427–9.

34. Jyoti J, Singh BP, Arya AK, Dhakate SR. Dynamic mechanical properties of multiwall carbon nanotube reinforced ABS composites and their correlation with entanglement density, adhesion, reinforcement and C factor. RSC Advances. 2016;6(5):3997–4006.

35. Barczewski M, Mysiukiewicz O, Andrzejewski J, Matykiewicz D, Medycki D, Kloziński A, et al. Thermo-mechanical and mechanical behavior of hybrid isotactic polypropylene glass fiber reinforced composites (GFRC) modified with calcium carbonate (CaCO3). Polymer Engineering and Science. 2020;60(7):1588–603.

36. Brostow W, Hagg Lobland HE, Narkis M. Sliding wear, viscoelasticity, and brittleness of polymers. Journal of Materials Research. 2006;21(9):2422–8.

37. Hejna A, Barczewski M, Andrzejewski J, Kosmela P, Piasecki A, Szostak M, et al. Rotational molding of linear low-density polyethylene composites filled with wheat bran. Polymers. 2020;12(5).

38. Matykiewicz D, Barczewski M. On the impact of flax fibers as an internal layer on the properties of basalt-epoxy composites modified with silanized basalt powder. Composites Communications. 2020;20:100360.

39. Deák T, Czigány T. Chemical Composition and Mechanical Properties of Basalt and Glass Fibers: A Comparison. Textile Research Journal. 2009;79(7):645–51.

40. Almond J, Sugumaar P, Wenzel MN, Hill G, Wallis C. Determination of the carbonyl index of polyethylene and polypropylene using specified area under band methodology with ATR-FTIR spectroscopy. E-Polymers. 2020;20(1):369–81.

41. Olinek J, Anand C, Bellehumeur CT. Experimental study on the flow and deposition of powder particles in rotational molding. Polymer Engineering & Science. 2005;45(1):62–73.

42. Duran J, Behringer RP. Sands, Powders, and Grains: An Introduction to the Physics of Granular Materials. Vol. 54, Physics Today. 2001. 63 p.

43. Khanam PN, AlMaadeed MAA. Processing and characterization of polyethylene-based composites. Advanced Manufacturing: Polymer and Composites Science. 2015;1(2):63–79.

44. Huang R, Xu X, Lee S, Zhang Y, Kim BJ, Wu Q. High Density Polyethylene Composites Reinforced with Hybrid Inorganic Fillers: Morphology, Mechanical and Thermal Expansion Performance. Materials. 2013;6(9):4122–38.

45. Khanna YP, Turi EA, Taylor TJ, Vickroy V V., Abbott RF. Dynamic mechanical relaxations in polyethylene. Macromolecules. 1985;18(6):1302–9.

46. Barczewski M, Hejna A, Kosmela P, Mysiukiewicz O, Piasecki A, Sałasińska K. High-density polyethylene – expanded perlite composites: structural oriented analysis of mechanical and thermomechanical properties. Materiale Plastice. 2022;59(3):52–63.

47. Mazur K, Jakubowska P, Romańska P, Kuciel S. Green high density polyethylene (HDPE) reinforced with basalt fiber and agricultural fillers for technical applications. Composites Part B: Engineering. 2020;202(July).

48. Gupta N, Ramkumar PL, Sangani V. An approach toward augmenting materials, additives, processability and parameterization in rotational molding: a review. Materials and Manufacturing Processes. 2020;35(14):1539–56.